An Efficient Approach to Modeling the Topographic Control of Surface Hydrology for Regional and Global Climate Modeling

MARC STIEGLITZ

Goddard Institute for Space Studies, New York, New York, and Department of Geological Sciences, Columbia University, New York, New York

DAVID RIND

Goddard Institute for Space Studies, New York, New York

JAMES FAMIGLIETTI

Department of Geological Sciences, University of Texas, Austin, Texas

CYNTHIA ROSENZWEIG

Goddard Institute for Space Studies, New York, New York

(Manuscript received 14 June 1995, in final form 12 June 1996)

ABSTRACT

The current generation of land-surface models used in GCMs view the soil column as the fundamental hydrologic unit. While this may be effective in simulating such processes as the evolution of ground temperatures and the growth/ablation of a snowpack at the soil plot scale, it effectively ignores the role topography plays in the development of soil moisture heterogeneity and the subsequent impacts of this soil moisture heterogeneity on watershed evapotranspiration and the partitioning of surface fluxes. This view also ignores the role topography plays in the timing of discharge and the partitioning of discharge into surface runoff and baseflow. In this paper an approach to land-surface modeling is presented that allows us to view the watershed as the fundamental hydrologic unit. The analytic form of TOPMODEL equations are incorporated into the soil column framework and the resulting model is used to predict the saturated fraction of the watershed and baseflow in a consistent fashion. Soil moisture heterogeneity represented by saturated lowlands subsequently impacts the partitioning of surface fluxes, including evapotranspiration and runoff. The approach is computationally efficient, allows for a greatly improved simulation of the hydrologic cycle, and is easily coupled into the existing framework of the current generation of single column land-surface models. Because this approach uses the statistics of the topography rather than the details of the topography, it is compatible with the large spatial scales of today's regional and global climate models. Five years of meteorological and hydrological data from the Sleepers River watershed located in the northeastern United States where winter snow cover is significant were used to drive the new model. Site validation data were sufficient to evaluate model performance with regard to various aspects of the watershed water balance, including snowpack growth/ablation, the spring snowmelt hydrograph, storm hydrographs, and the seasonal development of watershed evapotranspiration and soil moisture.

1. Introduction

With the increased recognition of the importance of feedbacks between land-surface processes and climate (Charney 1975; Charney et al. 1977; Lean and Warrilow 1989), as well as interest in the prediction of runoff and soil moisture under present and changed climate conditions (Manabe and Wetherald 1987; Rind et al. 1990; Miller and Russell 1992; Miller et al. 1994; Liston et al. 1994), there have been sustained efforts to develop more realistic land-surface representations for general circulation models (GCMs). In this paper we present an approach to land-surface modeling that allows us to view the fundamental hydrologic unit as the watershed rather than the soil column. The approach is computationally efficient, allows for a greatly improved simulation of the hydrologic cycle, and is easily coupled into the existing framework of the current generation of single soil column land-surface models.

Both models and data have shown that within a watershed substantial soil moisture heterogeneity exists at almost any scale (Bell et al. 1980; Owe et al. 1982; Wang et al. 1989) and that a major control on the distribution of soil moisture is topography (Beven and

Corresponding author address: Dr. Marc Stieglitz, Lamont Doherty Earth Observatory, Palisades, NY.

Kirkby 1979; Burt and Butcher 1985). Regions of local concavity (lowlands) tend to be zones of convergent flow (surface and baseflow) and, therefore, zones of high soil moisture content. In comparison, uplands soils tend to be progressively drier. Because of these topographic controls, the expansion and contraction of lowland saturated zones is predominantly determined by downslope redistribution of recharged subsurface soil water (i.e., infiltration minus evapotranspiration). When upland recharge is large, baseflow increases and lowland saturated zones expand. When recharge is small, baseflow decreases and lowland saturated zones contract. While the magnitude of baseflow is directly related to saturated regions of the watershed through upland recharge and topography, surface runoff, in many parts of the world, is also controled by the extent of the saturated regions (Hewlett and Hibbert 1965; Dunne and Black 1970; Freeze 1974). These saturated regions, in valleys and along hillslopes, represent the surface expression of the water table and, in sum, constitute the bulk of the saturated fraction of the watershed. In hydrologic literature this saturated fraction is referred to as the *partial contributing area* and direct overland flow resulting from precipitation over such saturated regions (Dunne runoff or saturation excess runoff) is a major contributor to surface runoff. Surface runoff resulting from infiltration excess over low permeability soils (Hortonian runoff) accounts for only a small fraction of the surface runoff contribution to streamflow. Therefore, the timing of the discharge (baseflow plus surface runoff) is dynamically linked to the overall state of the watershed water balance. Finally, the water and energy balance are coupled in that the distribution of soil moisture may play a significant role in the evolution of the surface energy balance. Evapotranspiration will be near the potential rate in saturated lowlands and falls off rapidly as one heads into drier uplands (Famiglietti and Wood 1994a,b).

However, land-surface models used in GCMs (Abramopoulos et al. 1988; Dickinson et al. 1986; Pitman et al. 1991; Pitman and Desborough 1996; Verseghy 1991) view the soil column as the fundamental hydrologic unit. These models prognostically calculate average soil moisture for each grid cell and from these values calculate surface fluxes, runoff, and infiltration of surface water. While this approach may be effective in simulating such processes as the evolution of ground temperatures and the growth/ablation of a snowpack at the soil plot scale (Lynch-Stieglitz 1994), it effectively ignores the role topography plays in the development of soil moisture heterogeneity and the subsequent impacts of this soil moisture heterogeneity on watershed evapotranspiration and the partitioning of surface fluxes. It also ignores the role topography plays in the timing of discharge and the partitioning of discharge into surface runoff and baseflow.

Recently there have been attempts to develop land-surface models for GCMs that do account for both the soil moisture heterogeneity and the subsequent effects on the generation of surface fluxes, runoff, and infiltration rates. Entekhabi and Eagleson (1989) use a two-parameter gamma probability density function (pdf) to represent the soil moisture distribution within a grid cell. From knowledge of the average grid cell soil moisture and the pdf, the saturated fraction of the watershed (partial contributing area) is calculated and surface runoff is partitioned into Dunne and Hortonian components. Furthermore, grid cell evapotranspiration is calculated not from the average grid cell soil moisture value but from soil moisture distribution about that value. While this scheme does generate the desired soil moisture heterogeneity, it has two main drawbacks. 1) The pdf representing the soil moisture distribution is not based on the site specific topography. As such, two grid cells with identical soil characteristics and driven by identical atmospheric forcing will evolve identically with respect to soil moisture, irrespective of the fact that the topography may differ in the two cells. 2) The scheme is not physically consistent in that the calculations yielding baseflow and the saturated fraction are independent.

The study of current and changed climates covering a wide range of climatic regimes requires a physically based model that will have the flexibility to deal with different conditions, whereas the spatial scales of regional and global climate models demands a computationally efficient model. In this vein, the advent of TOPMODEL, a conceptual rainfall–runoff model (Beven and Kirkby 1979; Beven 1986a,b; Beven et al. 1994), has provided hydrologists with a powerful tool to 1) analytically calculate the hillslope response of site specific topography without the need to resort to finite-element modeling and 2) operate at large watershed scales by using the statistics of the topography, rather than the details of the topography itself. The strong influence topography plays in the generation of watershed soil moisture heterogeneity and discharge characteristics forms the basis of TOPMODEL development. Prior to TOPMODEL, physically based hydrologic models required detailed simulation models that solved the partial differential equations governing water transport numerically. While this may be satisfactory at the scales of very small watersheds, it is computationally incompatible with the scales required by climate models. Making exactly this point, Wood et al. (1990) state ''a recent study of a small headwater catchment involving a 12 000-node simulation over a period of 150 days required a run time of 50 hours on a Cyber 205 supercomputer.'' Famiglietti and Wood (1991, 1994a) proposed the use of the TOPMODEL framework in the context of land-surface models to parameterize downslope redistribution of soil water and thus subgrid-scale spatial variability in the runoff and energy fluxes. While their TOPLATS (TOPMODEL-based Land–Atmosphere Transfer Scheme) parameterization is intended for use in climate models, its structure is presently not consistent with the stringent requirements for implementation in some GCMs (e.g., GISS GCM). It is dif-

ficult to merge this statistically based model in a discretized framework (see section 3b) with the physical transport of water and energy required by some GCMs. Further, the discretization itself is too computationally expensive for most GCM applications.

In this paper we present an approach to land-surface modeling that addresses these potential shortcomings while preserving the essence of the TOPMODEL formalism. The analytic form of TOPMODEL equations are incorporated into a single column model framework and the resulting model is used to predict the saturated fraction and baseflow in a consistent fashion. Soil moisture heterogeneity represented by saturated lowlands subsequently impacts the partitioning of surface fluxes, including evapotranspiration and runoff. While we couple TOPMODEL equations with a specific single column model, the procedure is general and could be applied to many of the single column representations now used in GCMs.

Model development proceeds in two stages. A single column land-surface model is developed that includes a new ground scheme, a three-layer snow model (Lynch-Stieglitz 1994), a modified BEST canopy model (Pitman et al. 1991; Pitman and Desborough 1996), and terrestrial-atmosphere radiation transfer calculations. While the single column model includes general hydrologic improvements to land-surface modeling; its basic philosophy is the same as current GCM land-surface models. Grid averaged values of soil moisture are used to generate surface fluxes, runoff, and infiltration rates. Topographic control on the soil moisture distribution is neglected. To account for topographic effects, an improved model is developed whereby TOPMODEL equations and Digital Elevation Model (DEM) data are coupled with the single-column model framework. The single-column model and the improved model are then used to simulate the hydrologic cycle at a small watershed located in the northeastern United States. In this fashion, not only can the new approach be evaluated, but the effects topography has on the generation of surface fluxes, runoff, and infiltration rates can be quantified.

The remainder of the paper is outlined as follows. Descriptions of both the single-column land-surface model and the improved model are given. A description of the site–validation data is given and the general characteristics and climatology of the watershed are discussed. Site-meteorological data are then used drive the models in an off-line mode, and validation data are used to evaluate model performance.

2. Single column model

A complete description of the single column model can be found in Lynch-Stieglitz (1995).

a. Ground model

The soil column is composed of six separate ground layers. Regardless of the actual depth to bedrock, we currently set the bottom of the deepest model layer at 3.0 m, 1 m beyond the maximum root depth for all seven vegetation types permitted. This eliminates problems in calculating the seasonal ground temperatures in regions with very shallow soils. For simplicity we choose a single soil texture class for the entire soil column. While it is possible to assign a separate texture class for each vertical layer (Abramopoulos et al. 1988), it is not felt such a breakdown is justified in the face of the great natural variability in soil texture found even within a small watershed. Resolution requirements dictate that in order to reasonably capture the diurnal range in the surface radiation temperature, layer 1 (surface layer) thickness can be no greater than the thermal damping depth of soil. As such, layer thicknesses are in a geometric series with the first ground layer taken to be 10 cm. Heat and water fluxes internal to the soil column are calculated as follows.

Heat transport within the soil column is governed by linear diffusion along the thermal gradient, heat carried into a layer by water infiltrating from above, and heat loss due to root water extraction and baseflow runoff. Because the seasonal temperature signal reaches beyond the depth of the lowest model layer, a lower boundary condition is imposed to account for the effects of the heat flux between the lowest model layer and the earth below (Lynch-Stieglitz 1994).

To account for both capillary suction and macropore flow (Beven 1982a), a modified tipping bucket model governs the water flux into a layer from the layer above (Da Silva and De Jong 1986). Until the water content of the layer above reaches 70% the field capacity (θ_{33}) (Table 1), flow is considered nonexistent (Hillel 1977). Above this level water drains at the gravitational rate, $K(\theta)$, where K is the hydraulic conductivity (m s^{-1}) and θ is the volumetric soil moisture. Following Brooks and Corey (1964), $K(\theta)$ in each model ground layer is calculated from the relevant soil parameters (Table 1) and modified by a freezing soil correction (Rawls and Brakensiek 1985). Upward movement of water due to capillary forces is neglected. The bottom of the sixth layer represents an ''impermeable basement'' to mass flow.

Heat and moisture fluxes couple the lower atmosphere and canopy to the ground surface. Once the heat and water fluxes have been determined, the heat and water content of each layer i can be updated, and the layer temperature, T_i, fraction of ice relative to the total water content in a layer, $f_{I,i}$, and total liquid water content in a layer, $W_{L,i}$, can be calculated. Rainfall (which carries heat) may hit the bare ground directly or reach the ground indirectly as throughfall in the vegetated fraction of the grid cell. The amount by which the precipitation rate exceeds the infiltration capacity of the surface soil, $I_{\max}$ (Abramopoulos et al. 1988), is surface runoff (R_s, m s^{-1}). The only other mechanisms that transfer water to or from the soil column are evaporation from layer 1, condensation onto layer 1, and root removal via transpiration. Finally, the maximum soil surface evaporation

TABLE 1. Soil water retention properties.

Texture class	Total† porosity ϕ $cm^3\ cm^3$	Residual water† content, θ_r $cm^3\ cm^3$	Effective† porosity, θ_e $cm^3\ cm^3$	Bubbling† pressure, h_b m	Pore-size† distribution γ	Water retained† at −33 kPa θ_{33} $cm^3\ cm^3$	Saturated‡ hydraulic conductivity, K_s, m s^{-1}
Sand	0.437	0.020	0.417	0.073	0.694	0.091	5.83×10^{-5}
Loamy sand	0.437	0.035	0.401	0.087	0.553	0.125	1.70×10^{-5}
Sandy loam	0.453	0.041	0.412	0.147	0.378	0.207	7.19×10^{-6}
Loam	0.463	0.027	0.434	0.112	0.252	0.270	3.67×10^{-6}
Silt loam	0.501	0.015	0.486	0.208	0.234	0.330	1.90×10^{-6}
Sandy clay loam	0.398	0.068	0.330	0.281	0.319	0.255	1.19×10^{-6}
Clay loam	0.464	0.075	0.390	0.259	0.242	0.318	6.39×10^{-7}
Silty clay loam	0.471	0.040	0.432	0.326	0.177	0.366	4.17×10^{-7}
Sandy clay	0.430	0.109	0.321	0.292	0.223	0.339	3.33×10^{-7}
Silty clay	0.479	0.056	0.423	0.342	0.150	0.387	2.50×10^{-7}
Clay	0.475	0.090	0.385	0.373	0.165	0.396	1.67×10^{-7}

† Rawls et al. (1993).
‡ Rawls et al. (1982).

rate (exfiltration rate) is modeled according to Gardner and Hillel (1962).

b. Snow model

When the surface air temperature, T_a, is less than 0 degrees Celsius, precipitation falls as snow, and the snow cover is presumed to cover the entire ground surface. In previous work (Lynch-Stieglitz 1994), a simple snow model was developed and incorporated into an off-line modified version of the GISS land-surface scheme (Abramopoulos et al. 1988). A 5-yr record of meteorological and hydrological data from a snow research station (1969–74) located within the Sleepers River watershed (see section 4a) was used to drive and validate the model. Site validation data demonstrated that not only are the radiation temperatures of the ground and snow surface adequately modeled, but all the features of snowpack ripening that characterize pack growth/ablation are simulated. It is this snow model that is incorporated into our new land-surface scheme.

The snowpack is modeled with three snow layers. Heat and mass (water) flow within the pack are explicitly modeled. Radiation conditions determine the surface energy fluxes, and since meltwater by definition carries no heat, the heat flow within the pack is accomplished solely via linear diffusion along the thermal gradient. Each snow layer is characterized by a volumetric water holding capacity. As such, meltwater generated in a layer will remain in the layer if the liquid water content of the layer is less than the layer holding capacity. Otherwise, it will flow down to a lower layer where it will either refreeze in the layer, remain in the layer in the liquid state, or pass through. Two independent processes govern densification of the pack. A simple parameterization is used to describe mechanical compaction or compaction due to the weight of the overburden, and a separate densification is accomplished via the melting–refreezing process.

One modification made to the Lynch-Stieglitz (1994) snow model is that the snowpack albedo is now explicitly modeled. Following Hansen et al. (1983), snowpack albedo is parameterized as a function of snow surface aging where a fresh snow albedo of 0.85 decays to a value of 0.5 with a 50-day timescale.

c. Canopy model

The canopy model developed for the BEST land-surface model (Pitman et al. 1991; Pitman and Desborough 1996) is adopted and modified. While a detailed description of the BEST canopy model can be found in Pitman et al. (1991), it should be noted the scheme is conceptually similar to that developed for the BATS (Dickinson et al. 1986) land-surface model. The physical characteristics that represent the vegetation in the BEST canopy model are the leaf area index (LAI), stem area index (SAI), and the root distribution. The LAI varies seasonally as a function of the deeper ground temperatures. Following Deardorff (1978), a water-holding capacity is defined for the canopy as a function of the combined LAI and SAI. Precipitation over the vegetated fraction hits the canopy and falls through to the ground if the water-holding capacity of the canopy is exceeded. Dew formation onto the canopy is treated similarly. Transpiration results in a loss of water from the soil column via root removal. Following Deardorf (1978) and Dickinson et al. (1986), the canopy resistance is a function of the LAI, canopy temperature, the partitioning of the solar radiation between the upper and lower canopy, a light sensitivity factor (unique for each vegetation class), and the minimum and maximum stomatal resistances. Root resistance to flow is dependent on the root distribution in the soil column and the state of the soil moisture.

With regard to the physical characteristics of the canopy model, the following changes to the BEST canopy model were implemented. 1) To generate the seasonal

ground temperature used to calculate LAI, temperatures in layers 4, 5, and 6 are weighted by 0.5, 0.333, 0.167, respectively, and summed. 2) The root-distribution scheme of Abramopoulos et al. (1988) is used and the BEST root-resistance formulation is adapted accordingly. 3) A new parameterization is developed for the canopy water-holding capacity based on storage coefficients specific to the vegetation type (Ripley and Redman 1975; Calder 1990, 1993). 4) It has been proposed that the high canopy resistance values observed in forests (approximately four times that of grasslands; Szeicz and Long 1969; Stewart and Thom 1973; Monteith 1975a, b; Lindroth 1985; Shuttleworth 1989) reflects the ability of forests to preserve water in the face of a turbulent atmosphere with a high vapor pressure deficit (Monteith 1975b; Calder 1993; Lindroth 1993). While not explicitly modeling the vapor pressure deficit dependence, we empirically account for these observations by assigning a higher minimum stomatal resistance to forests. See Lynch-Stieglitz (1995) for a detailed discussion.

Within the vegetated fraction of the grid cell, the canopy freely radiates to the atmosphere and interacts with the ground surface directly below the canopy through a radiative exchange. The sensible and latent heat fluxes between the canopy and the atmosphere, and the ground surface directly below the canopy and the atmosphere, are mediated through an exchange with the air internal to the canopy. Because the canopy is assumed to have zero heat capacity, the canopy heat balance requires that the canopy temperature be solved for iteratively. In effect, this iterative solution also solves for the temperature and relative humidity of the air internal to the canopy, the canopy fluxes, and the fluxes from the ground surface directly below the canopy simultaneously. A detailed description of the formulations used are given in the BEST documentation. With regard to the canopy–atmosphere radiation balance, the following change to the BEST model was implemented. Precipitation that lands on the canopy and water that flows to the canopy from the root zone transfers heat to the canopy. Terms that account for these transfers of heat were added to the canopy energy balance. This change was made to impose strict mass and energy balance for the land-surface model, a necessary prerequisite for inclusion in some general circulation models.

d. Terrestrial–atmosphere radiation transfer

The surface terrestrial scheme includes a surface radiation scheme and surface flux calculations. The general approach taken here follows that of the BEST model (Pitman et al. 1991). One reason for following this approach is that a common soil column underlies both the bare and vegetated fractions. This allows for the easy incorporation of topographic effects into the model since the soil column can be thought of as a continuum where convergent horizontal flow links lowland saturated zones to upland recharge (section 3). Models employing multiple soil columns representing the various fractions of the grid cell permit no such easy connectivity between lowland and upland regions (Abramopoulos et al. 1988; Koster and Suarez 1992). However, unlike the BEST model, we do not incorporate the concepts of self similarity into this terrestrial scheme.

While three basic land covers are allowed (bare soil, snow, and vegetation), the grid cell is divided into two fractions: a vegetated fraction (A_v) and a nonvegetated fraction (A_u). In the presence of snow, it is presumed the ground surface is entirely snow covered and that a fraction of the green vegetation is masked by the snow (Hansen et al. 1983). The nonvegetated fraction (A_u) then becomes that portion of the grid cell where vegetation is not visible, including the formerly bare soil fraction and the masked vegetation fraction.

Following Pitman et al. (1991), we assume the surface albedo can be equally partitioned between the visible (≤ 0.7 μm) and the near IR (>0.7 μm) spectrum. The grid cell albedo is then the weighted average of the albedo for the vegetated fraction and the albedo for the bare ground fraction. In the absence of snow the bare ground albedo as specified in Table 2 is reduced according to the water content in the surface ground layer (Hansen et al. 1983). In the presence of snow, the bare ground albedo is replaced by the snow albedo.

The neutral drag coefficient, C_{DN}, is calculated from the grid cell roughness, z_0, and related to the atmospheric stability through the Richardson number to arrive at the drag coefficients for heat (C_{Dh}), vapor (C_{Dv}), and momentum (C_{Dm}), where $C_{Dh} = C_{Dv}$. The detailed formulations of C_{Dh}, C_{Dv}, and C_{Dm} found in Pitman et al. (1991) follow Boer et al. (1984) and McFarlane and Laprise (1985).

Within each grid cell up to eight land covers may be specified in varying fractions. As shown in Table 2, each vegetation class is associated with unique values of albedo, snow-masking depth (d_s^*), roughness length (z_0), leaf area index (LAI) parameters, etc. However, as grid cell calculations require grid cell values, vegetation parameters must be composited in some manner. Then A_v becomes the snow-free sum of land-cover fractions two through eight. For each of the eight land covers snow-free albedos are calculated at a given Julian date by linearly interpolating albedo values shown in Table 2. From the fractional weighting of each vegetation class specified within a grid cell, the snow-masking fraction for each vegetation, and land-cover albedos, grid cell values of albedo, A_v, LAI, etc., are then calculated. Finally, the Pitman et al. (1991) formulation for the grid cell roughness, z_0, is appropriately composited.

Incoming radiation is partitioned between the bare and vegetated fractions. From the albedos of each fraction, the direct radiative forcing of the bare and vegetated surfaces are calculated. The soil surface in the bare fraction of the grid cell freely radiates to the atmosphere and exchanges sensible and latent heat fluxes with the surface layer through bulk aerodynamic formulations.

TABLE 2. Vegetation characteristics.

		1 Desert	2 Tundra	3 Grass	4 Shrub	5 Woodland	6 Deciduous	7 Evergreen	8 Rain forest
Visual albedo†	Winter	0.35	0.07	0.09	0.09	0.08	0.1	0.07	0.06
	Spring	0.35	0.06	0.1	0.1	0.07	0.05	0.07	0.06
	Summer	0.35	0.08	0.09	0.14	0.08	0.06	0.08	0.06
	Autumn	0.35	0.08	0.09	0.11	0.06	0.05	0.06	0.06
Near-IR albedo†	Winter	0.35	0.2	0.27	0.27	0.23	0.3	0.2	0.18
	Spring	0.35	0.21	0.35	0.3	0.24	0.22	0.2	0.18
	Summer	0.35	0.3	0.36	0.42	0.3	0.29	0.25	0.18
	Autumn	0.35	0.25	0.31	0.33	0.2	0.22	0.18	0.18
Masking depth, d_s*, (m)†		0.1	0.2	0.2	0.5	2	5	10	25
Roughness length, z_o, (m)‡		0.01	0.06	0.1	0.1	0.1	1	1	1
Max. leaf area index, LAI_{max}‡		0	4	3	4	4	6	6	6
Potential seasonal range of LAI, S_l‡		0	3.5	2.5	3.5	3.5	5.5	1	5.5
Stem area index *SAI*‡		0	0.5	1	1.5	1.5	2	2	2
Minimum stomatal resistance, r_{smin} (m s^{-1})		NA	17	17	17	17	111	111	111
Canopy water storage coefficient, *a(i)*		0	0	0.1	0.13	0.13	0.15	0.11	0.11
Photosynthetic factor, f_c‡		0	0.01	0.01	0.01	0.01	0.03	0.03	0.03

† Hansen et al. (1983).
‡ Pitman et al. (1991).

The top snow layer, and not the ground surface, determines surface fluxes when snow is present.

This single-column model generates grid-cell-averaged values for leaf temperature (T_c), ground temperatures (T_i), and ground soil moistures (θ_i), from which grid-cell-averaged fluxes may be generated. As demonstrated in Lynch-Stieglitz (1994), modeling only the vertical fluxes of water and energy within a single-column framework may be sufficient when validating snowpack growth–ablation and the evolution of ground and snow temperatures at the plot level. However, if the concern is the representation of topographically generated processes, this approach to watershed modeling is inappropriate. The next section describes the incorporation of TOPMODEL equations into this modeling framework.

3. Incorporation of TOPMODEL equations

a. TOPMODEL description

TOPMODEL formulations allow for the dynamically consistent calculations of both the saturated fraction of the watershed and the baseflow that supports that saturation from knowledge of the mean watershed water table depth and a probability density function (pdf) of combined topographic and soil properties. At the core of TOPMODEL are three basic assumptions: 1) The water table is nearly parallel to the soil surface so that the local hydraulic gradient is close to tan β, where β is the local slope angle. 2) The saturated hydraulic conductivity, K_s, declines exponentially with depth

$$K_s(z) = K_s(z = 0)e^{-fz}, \tag{1}$$

where f is the saturated hydraulic conductivity decay factor and z is depth (positive downward). 3) At depth the water table is recharged at a spatially uniform and steady rate with respect to the response timescale of the watershed. As such, recharge and baseflow are balanced in a series of steady states. From these three assumptions it can be shown that an analytic relation exists between the mean water table depth ($\bar{z}$) and local water table depth at any location $x(z_x)$ within the watershed. This equation is approximated by

$$z_x = \bar{z} - 1/f[\ln(a/\tan\beta)_x - \Lambda] \tag{2}$$

[see Sivapalan et al. (1987) for the exact form of the equation], where the term $\ln(a/\tan\beta)_x$ is defined to be the topographic index χ whose ratio is a measure of the area above any point in the catchment that drains through the unit contour at location $x(a)$ (a measure of how much water can potentially flow through this location) to the local slope at that point (tan β) (a measure of how fast water can be transported downslope through this location), and Λ is the mean watershed value of $\ln(a/\tan\beta)$. By setting z_x equal to zero in Eq. (2) it is seen that all locations x associated with values of the topographic index χ greater than $\Lambda + f\bar{z}$ are within saturated regions. Finally, integrating Eq. (2) along the watershed channel network (Sivapalan et al. 1987) yields the baseflow (R_b, m s^{-1})

$$R_b = \frac{K_s(z = 0)}{f}e^{-\Lambda}e^{-f\bar{z}}. \tag{3}$$

Equations (2) and (3) comprise the basic formulations that govern flow beneath the water table and the distribution of the water table with respect to the topography. From knowledge of $\bar{z}$ and the cumulative distribution of

the topographic index χ (obtained from DEM data), the fraction of the watershed that is saturated and the baseflow consistent with this fraction can be calculated. A complete description of TOPMODEL can be found in Beven and Kirkby (1979) and Beven (1986a,b). Computation of the $\ln(a/\tan\beta)$ distribution from basinwide DEM data and discussions regarding the effects that DEM data resolution has on model results can be found in Wolock and McCabe (1995), Quinn et al. (1995), Wolock and Price (1994), and Zhang and Montgomery (1994).

b. *Application and incorporation of TOPMODEL framework*

Typically, the distribution of $\ln(a/\tan\beta)$ is discretized into a number (10–50) of intervals, each representing that fraction of the watershed with similar water table depth and soil moisture characteristics. Water and energy balance equations are applied at each interval, and separate estimates of unsaturated zone soil moisture, evapotranspiration, and runoff are calculated for each interval (Famiglietti and Wood 1994a,b; Wolock and Price 1994). The individual fluxes are then areally weighted and combined to obtain the water balance for the entire watershed. Famiglietti and Wood (1994a,b) show that with this approach the spatial variations in surface fluxes (high evapotranspiration and surface runoff from lowland saturated regions and low evapotranspiration and surface runoff from drier upland regions) are well simulated. While this approach is effective, the discretization would add much computation time to a land-surface model for regional or global climate models, as each grid cell must be discretized into a number of intervals. In addition, it is difficult to merge this statistically based model in the discretized flamework with the physical transport of water and energy required by some GCMs.

In order to preserve the essence of the TOPMODEL equations while satisfying the demands of a GCM, we take a different approach to adding a realistic water balance to the equations of Beven and Kirkby (1979). Instead of discretizing (which adds computation time) we couple the analytic form of the TOPMODEL equations with the single-column land-surface model that tracks the mean state of the watershed. From an update of the mean water table depth ($\bar{z}$), TOPMODEL equations and DEM data are used to generate baseflow [Eq. (3)] and the saturated fraction of the watershed. The partitioning of the watershed between saturated and unsaturated zones is now consistent with the estimate of baseflow within the framework of the TOPMODEL equations. Evapotranspiration, surface fluxes, and surface runoff is then calculated separately for the saturated and unsaturated fractions of the watershed. The subsequent fluxes are then combined to update the mean state of the single-column model. While diminishing the computation time significantly, the calculation of the fluxes based on the division of the watershed into two zones (saturated and unsaturated) will not necessarily provide us with as realistic fluxes as the traditional application of TOPMODEL where the watershed is discretized into many zones. Figure 1 depicts schematically the application of TOPMODEL equations. A formal description of the coupling of TOPMODEL equations with the single-column model follows.

1) THERMAL REGIME

Although we now partition surface evaporation and transpiration between saturated and unsaturated fractions of the grid cell, those processes described in section 2 that govern heat transport between model layers and the heat flux to the atmosphere remain the same.

2) MOISTURE REGIME

(i) Soil hydraulic properties. The validity of the assumption of exponential decay of the saturated hydraulic conductivity with depth is supported by data from Beven (1982b, 1984) and Elsenbeer et al. (1992). Increased biological activity and mechanical action near the soil surface, especially in vegetated regions, results in a near surface zone characterized by a preponderance of macropores and channels that represent easy flow pathways to infiltrating water. As such, the effective saturated hydraulic conductivity, K_s, of the near surface is extremely high relative to the ''compacted'' near bedrock values typically found in laboratory tests. We calculate the exponentially decaying K_s for the model as follows. The value for the surface saturated conductivity, $K_s(z = 0)$, is taken from Beven (1982b), which gives values based on soil texture and vegetation cover. At a depth of 25% beyond the maximum root depth it is assumed the saturated conductivity has reached the compacted value that is taken from Rawls et al. (1982) (Table 1). The saturated conductivities at the midpoints of the six model layers, $K_{s,i}$, are then calculated assuming an exponential decrease of conductivity with depth [Eq. (1)]. This impacts infiltration characteristics through the calculations for $I_{\max}$ and $K_i(\theta)$ (see section 2a). We also use this information to calculate the decay factor, f [Eq. (1)], which is needed for the TOPMODEL calculations.

(ii) Saturated fraction of the grid cell. To calculate that fraction of the watershed that is saturated (the partial contributing area), f_{sat}, requires the cumulative pdf of the topographic index χ and the mean water table depth $\bar{z}$. Starting at the bottom of the soil profile, $\bar{z}$ is located within the first unsaturated layer i such that

$$\bar{z} = zb_i \qquad \theta_i \le 0.7\theta_{33}$$

$$\bar{z} = zb_i - \left(\frac{\theta_i - 0.7\theta_{33}}{\phi - 0.7\theta_{33}}\right)\Delta z_i \qquad \theta_i > 0.7\theta_{33}, \quad (4)$$

where zb_i is the bottom boundary of model layer i. Term f_{sat} is then calculated to be the cumulative area under

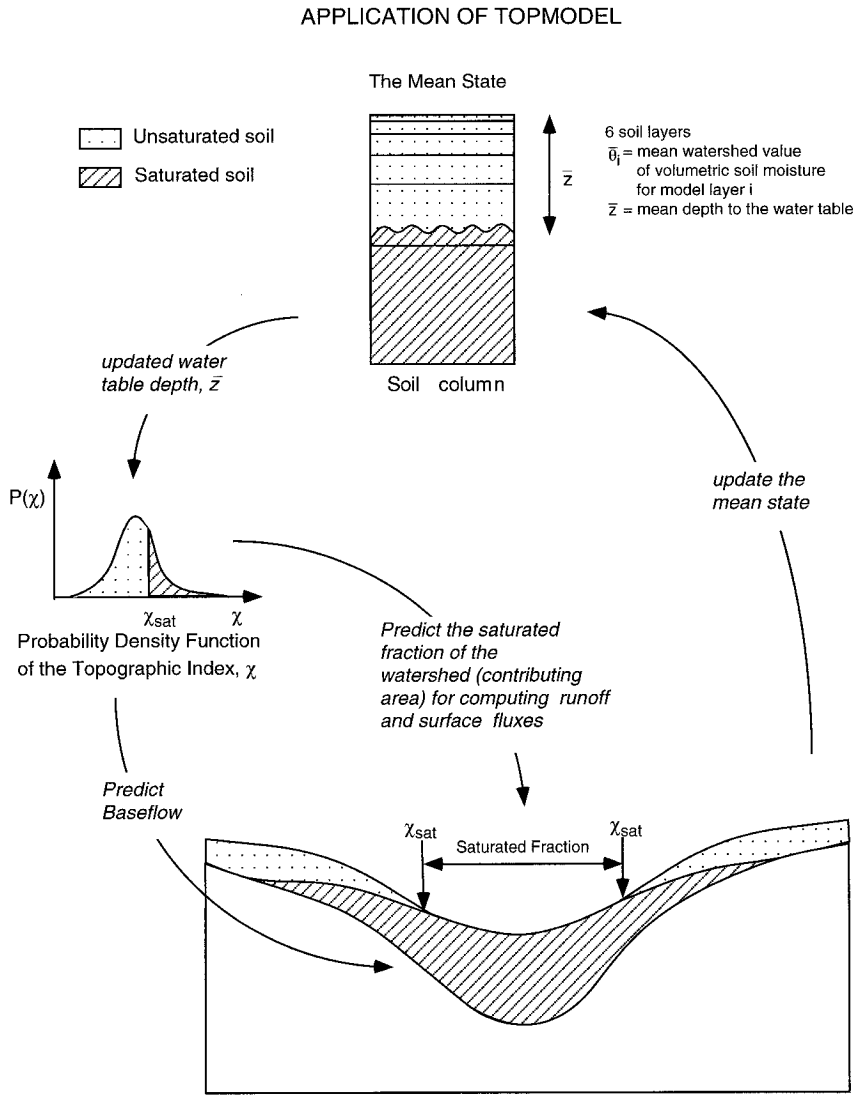

FIG. 1. Coupling the analytic form of TOPMODEL equations with the single column model. From an update of the mean water table depth ($\bar{z}$), TOPMODEL equations and DEM data are used to generate baseflow [Eq. (3)] and the saturated fraction of the watershed.

the pdf with values of the topographic index χ greater than $\Lambda + f\bar{z}$ (see Fig. 1). If model layer 6 is unsaturated, (i.e., $\bar{z} > zb_6$), f_{sat} and baseflow (R_b) are taken to be zero.

(iii) Soil moistures within the region $(1 - f_{\text{sat}})$. The vertical movement of liquid water within the soil column, the maximum infiltration capacity, $I_{\max}$, the maximum soil surface evaporation rate, and evapotranspiration in the unsaturated fraction of the grid cell are calculated not from the mean grid cell values of volumetric soil moistures but from the calculated values of soil moisture for the unsaturated region. The volumetric soil moistures in the unsaturated fraction of the grid cell are calculated by assuming the mean watershed value of the volumetric soil moisture, θ_i, is a weighted average of the soil moisture for the unsaturated zone, $\theta_{u,i}$, and that of the saturated zone, which is simply the porosity, ϕ:

$$\theta_{u,i} = \frac{\theta_i - f_{\text{sat}}\phi}{1 - f_{\text{sat}}}. \tag{5}$$

iv) Runoff. Surface runoff, R_s, is modeled according to

$$R_s = (1 - f_{\text{sat}})\xi_1 + f_{\text{sat}}\xi_2,$$

where

$$\xi_1 = A_u \max(Pr - I_{\max}, 0) + A_v \max(Dr - I_{\max}, 0)$$

$$\xi_2 = A_u Pr + A_v Dr \in \text{the absense of snow cover}$$

or

$$\xi_1 = \max(Sm - I_{\max}, 0)$$

$$\xi_2 = Sm \in \text{the presence of snow cover}, \quad (6)$$

where Sm (m s^{-1}) is the melt rate from the bottom of the snowpack, Pr (m s^{-1}) is the precipitation rate, and Dr (m s^{-1}) is the canopy drip rate. The term $(1 - f_{\text{sat}})\xi_1$ represents runoff resulting from rates of precipitation, throughfall, and snowmelt over unsaturated regions that exceed the maximum infiltration capacity, $I_{\max}$ (Hortonian runoff). The term $f_{\text{sat}}\xi_2$ represents runoff resulting from precipitation, throughfall, and snowmelt over saturated regions (Dunne runoff). To conserve mass and energy, the contribution to runoff from condensation is also accounted for. Total baseflow, R_b [Eq. (3)], is partitioned among the six model layers according to

$$R_{b,j} = \left[\frac{K_{s,j}(zb_j - \bar{z})}{K_{s,j}(zb_j - \bar{z}) + \sum_i^6 K_{s,i}\Delta z_i} \right] R_b$$

j = the model layer that contains the water table

and

$$R_{b,i} = \left[\frac{K_{s,i}\Delta z_i}{K_{s,j}(zb_j - \bar{z}) + \sum_i^6 K_{s,i}\Delta z_i} \right] R_b \qquad i = j + 1, 6, \quad (7)$$

where the baseflow contribution from model layers within or below the water table is weighted by the saturated conductivity of the layer times the amount of water in the layer. Due to the exponential decrease of saturated conductivity with depth, water in the lower saturated model layers have a longer residence within the soil column than waters residing in the upper saturated layers.

3) SURFACE FLUXES

With the addition of topographically generated subgrid-scale soil moisture we modify the single-column model calculation of surface evaporative fluxes from the bare fraction of the grid cell such that

$$E_b = [f_{\text{sat}} + \beta(\theta_{u,1}, T_1)(1 - f_{\text{sat}})]E_p, \quad (8)$$

where

E_b bare ground evaporative flux within A_u (m s^{-1}),

E_p bare ground potential evaporation rate within A_u (m s^{-1}),

$\beta(\theta, T)$ evaporative efficiency factor.

Formulations for E_p and $\beta(\theta, T)$ are given in Pitman et al. (1991). While the partitioning of evaporative surface fluxes between saturated and unsaturated regions impacts the calculation of T_1 through the surface energy balance, there is no similar way to partition T_1, and therefore sensible and longwave surface fluxes are strictly a function of T_1, the mean watershed value. As f_{sat} represents the surface expression of the water table, evaporative fluxes from f_{sat}, removes water from the layer that contains the water table. Evaporative fluxes from unsaturated regions removes water from model layer 1. Likewise, the single-column formulations used to generate surface fluxes from the ground beneath the canopy and the canopy itself (located in the vegetated fraction of the grid cell, A_v) are appropriately modified to account for the partitioning of soil moisture between saturated and unsaturated regions.

c. Model stability and time step

Although the meteorological data used to drive the model are input hourly, the energy fluxes at the ground and snow surface mainly determine the model's internal time step. During the five seasons modeled, the model-determined (topographic effects included) time step averaged 22 min. The total run time for the model was approximately 5 min on a 486 66 MHz PC. As a reference point for GCM models, this total run time is virtually identical to that when using a current off-line working version of the GISS land-surface model (Abramopoulos et al. 1988).

4. Model validation

a. Sleepers River watershed data

This section summarizes an extensive discussion on the Sleepers River watershed given in Anderson (1977).

The Sleepers River Watershed (111 km^2) located in the glaciated highlands of Vermont is hydrologically representative of most upland regions in the northeast United States. As such, this site was chosen in 1957 as an experimental watershed by the Agricultural Research Service (ARS) to provide a better understanding of natural watershed behavior and aid in the development of testing physically based hydrologic models (Anderson 1977).

Nested entirely within the Sleepers River Watershed is the W-3 subwatershed (8.4 km^2). It is five years of meteorological and hydrological data taken in this watershed between 1969–74 that is used to drive and evaluate our land-surface models. The W-3 topography is characterized by rolling hills and the predominant soils are silty loams. Land cover is approximately one-third grassland, one-third coniferous forest, and one-third deciduous forest; the watershed drains into the Pope Brook. At the southwest boundary of W-3 is the (National Oceanic and Atmospheric Administration)

TABLE 3. Summary of input validation datasets available for the Sleepers River W-3 watershed.

Variable	Description
Input dataset: Period of record = November 1969–August 1974	
Air temperature (°C)	Hourly, taken at 1-m height
Mean areal precipitation (m)	Hourly, taken at 1-m height
Dewpoint temperature (°C)	Hourly, taken at 1-m height
Wind speed (m s^{-1})	Hourly, taken at 1-m height
Incoming solar (W m^{-2})	Hourly, taken at 1-m height
Incoming longwave (W m^{-2})	Hourly; estimated from Anderson (1967) and clear-sky data for site (obtained from Anderson)
Validation dataset: Period of record = November 1969–August 1974 at the snow research station	
Snow height (m)	Variable (daily to every few days)
Snowpack water equivalent (m)	Variable (daily to every few days)
Snow surface temperature (°C)	Variable (usually twice daily, 0600 and 1800 LT, sometimes hourly)
Snowpack temperatures (°C)*	Taken at 6, 12, 24, and 36 inches above ground–snow interface, twice daily (0600 and 1800 LT)
Ground temperatures (°C)	Taken at 3, 6, 12, 24, and 36 inches below ground surface, twice daily (0600 and 1800 LT)
At the Pope Brook weir	
Discharge (m^3 s^{-1})	Hourly

* November 1969–May 1973 only.

NOAA-ARS snow research station, a 15-acre clearing that at best can be described as grassland. Initiated in 1966 to collect a set of sufficiently high resolution hydro-meteorological measurements that could be used to better understand snowpack growth–ablation and to evaluate complex snow models, this research station records all relevant meteorological parameters on an hourly basis (Anderson 1976). At an altitude of 552 m, the snow station's mean annual air temperature of 4.1°C with a standard deviation of 11.4°C is fairly representative of the watershed as a whole. The mean annual precipitation for the W-3 watershed is about 109 cm. The maximum water-equivalent snow depth is normally about 23–30 cm and the total snow depth averages about 254 cm. Snow cover usually persists from December to March with snowmelt in late March and April. The dominance of the snowpack as the single greatest store of yearly water is clearly reflected in the spring hydrograph.

It is the 5-yr record of hydro-meteorological measurements taken within W-3 (Table 3) that will be used to evaluate the land-surface models. Two datasets are shown in Table 3. The first is the required hourly input variables needed to drive the land-surface model in an off-line mode. At the snow research station hourly values of air temperature, dewpoint temperature, incident solar and thermal radiation, and wind speed are recorded. Mean areal precipitation is calculated from measurements taken at the seven raingauges located throughout W-3 (Anderson 1977). The second will be used to validate model results. Snow station validation measurements include ground temperatures, snow depth, snow water equivalent, and snow temperatures at the snow surface and at fixed depths within the pack. A weir located where the Pope Brook exits W3 records hourly discharge. DEM data for W-3 is available at a resolution of 30 m $\times$ 30 m.

b. Model soil profile and initial conditions

In order to run the land-surface model in an off-line mode, information other than the meteorological input data of Table 3 is required. Soil information must be specified so that soil hydraulic properties can be determined. Likewise, the 1 November 1969 initial conditions for soil moisture and layer temperatures must be given. The predominant soil at the W-3 watershed is silty loam (USDA 1993). Surface pressure at the site is taken to be 950 mb, the mean station value. Initial volumetric moisture was set to saturation and initial ground temperatures were estimated from the long-term air temperature record at the site and the solution of the diffusion equation over a semi-infinite halfspace with respect to a silty loam soil. The model soil profile with the 1 November 1969 ground moisture and temperatures is shown in Fig 2. For single-column runs, the mean depth to bedrock, taken at 3 m, is not only consistent with the full topographic model but also with site data and the FAO database (1974). So that the meteorological forcing data is consistent with site land cover, the watershed is modeled as 100% grassland, rather than a one-third grassland, one-third deciduous forest, and one-third coniferous forest composite. While this may impact overall water-energy balance, it is not possible to use the wind and humidity measurements collected at a height of 1 m at the snow research station (a grassy

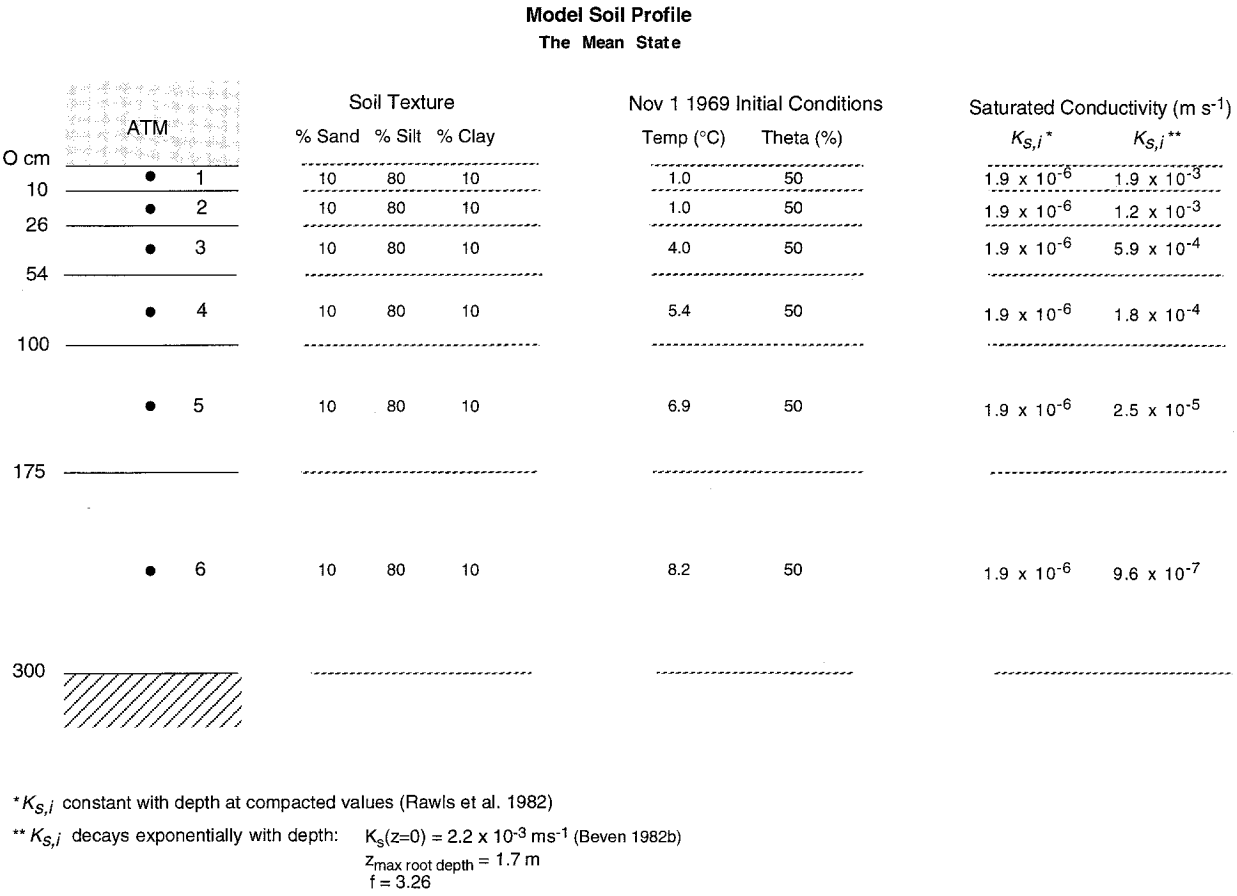

FIG. 2. Model soil profile and 1 November 1969 initial conditions for soil temperature and moisture. Theta is the volumetric soil moisture.

field) to drive a forest canopy. Theory could allow us to extrapolate these values to a greater height, but the uncertainties in this extrapolation are at least as large as the error introduced by using the incorrect vegetation type for the watershed. To allow the model to adjust for initial conditions, validation with site data begins 1 January 1970. The statistics of the topographic index χ were calculated from 30 m $\times$ 30 m DEM data using the multiple-flow direction algorithm outlined in Wolock and McCabe (1995). From these statistics and a three parameter gamma distribution the cumulative pdf of the topographic index χ was obtained.

Following Lynch-Stieglitz (1994) we generate the 1 November 1969 initial condition for the temperature of the deep, T_d, for both the single-column model and the improved model. The fact that T_d determined in this manner is approximately 2.5°C greater than the long-term air temperature (for both models) reflects the asymmetric nature of snowpack insulation whereby the ground is insulated from the atmosphere only in winter.

c. Model results

To evaluate the effects topography has on the generation of surface fluxes, runoff, infiltration rates, ground temperatures, and the growth/ablation of the snowpack, the full five years of hydro-meteorological data are now used to drive and evaluate our land-surface models. Three separate model runs are analyzed; two model runs with the single-column model and one run with the improved model where TOPMODEL equations and the single-column model are coupled as shown in Fig. 1. When running the single column model alone we include the subsurface runoff scheme of Abramopoulos et al. (1988) in the model structure. This allows for some representation of baseflow in these runs. In the Abramopoulos et al. (1988) scheme, subsurface runoff is directly related to the hydraulic conductivity of a layer and the mean grid cell surface slope [taken to be 6°C; FAO database (1974)], and inversely related to an interstream distance (taken to be 100 m). First we run the single-column model (including the Abramopoulos et al. subsurface runoff), where $K_{s,i}$ are taken to be constant with depth. In this run values for $K_{s,i}$ are the soil compacted values (Table 1), and as such, the model configuration is similar to most land-surface models used in today's GCMs. As an intermediate step to fully incorporating for topographic effects, the second run incorporates the exponential decline of $K_{s,i}$ (as described in section 3b (2)(i) into the above single column model.

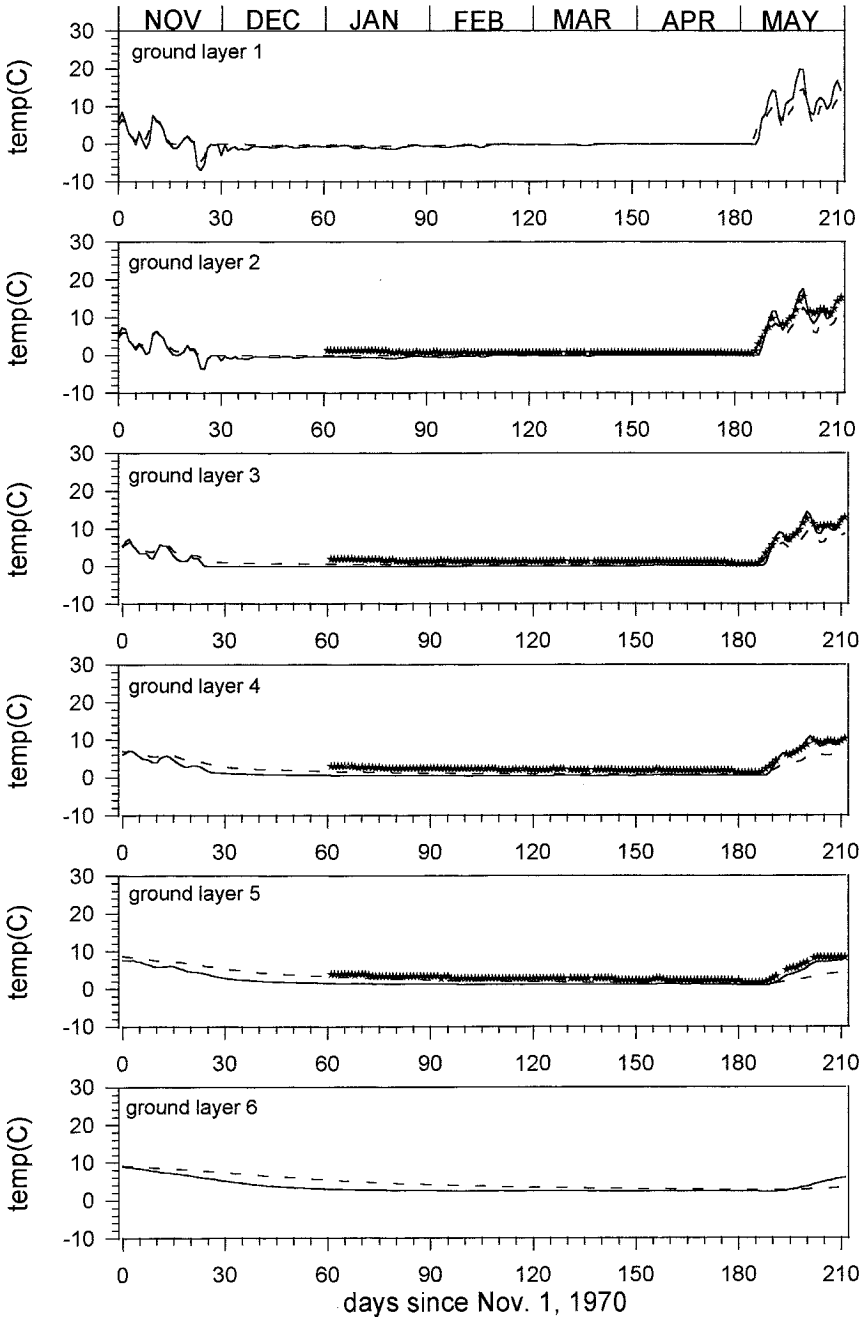

FIG. 3. Model-predicted (the improved model which incorporates TOPMODEL equations) daily averaged ground temperatures for the 1970/71 snow season and ground temperature data observed at the NOAA-ARS snow research station: ★★★ = site data; — = model results with nonvegetated, sandy soil condition found at the snow research station; – – – = model results with 100% grassland and soils representative of W-3 watershed (see Fig. 2).

This intermediate run allows us to examine the sensitivity of the single-column model to the exponential distribution of $K_{s,i}$ assumed in TOPMODEL. Finally, the full topographic model is run where TOPMODEL equations are coupled to the single-column model as described in section 3. We will show that only by including this full TOPMODEL construct do we substantially improve runoff. The model soil profile and the associated $K_{s,i}$ for each of the model runs are shown in Fig. 2.

Spring meltwater derived from the winter snowpack represents a major source for the yearly ground moisture budget at Sleepers River, and modeling the regional hydroclimatology is therefore predicated upon correctly

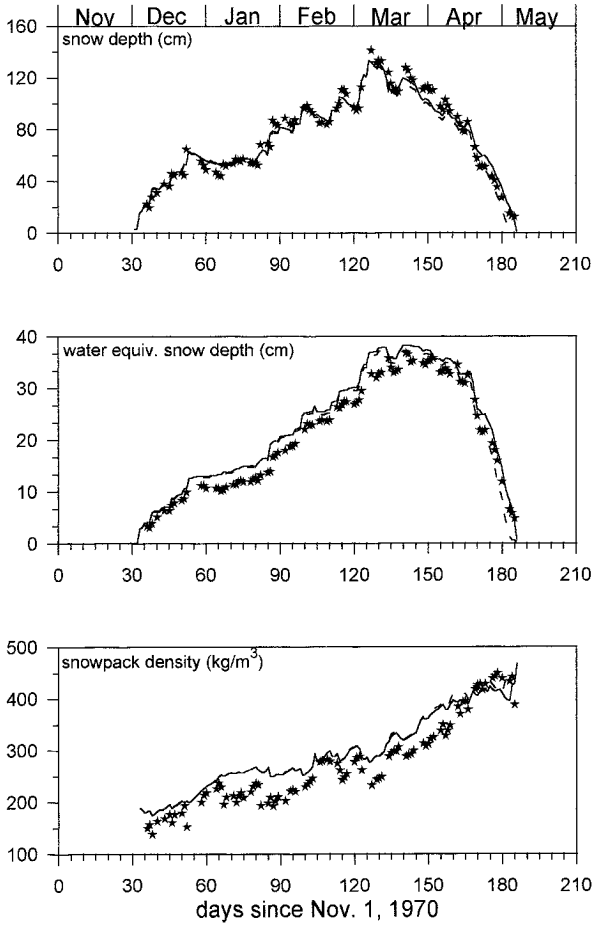

FIG. 4. Model-predicted (the improved model which incorporates TOPMODEL equations) snow depth, water equivalent snow depth (mass), and snowpack density for the 1970/71 snow season and observed snow characteristics at the NOAA-ARS research station: ★★★ = site data; — = model results with nonvegetated, sandy soil condition found at the snow research station; – – – = model results with 100% grassland and soils representative of W-3 watershed (see Fig. 2).

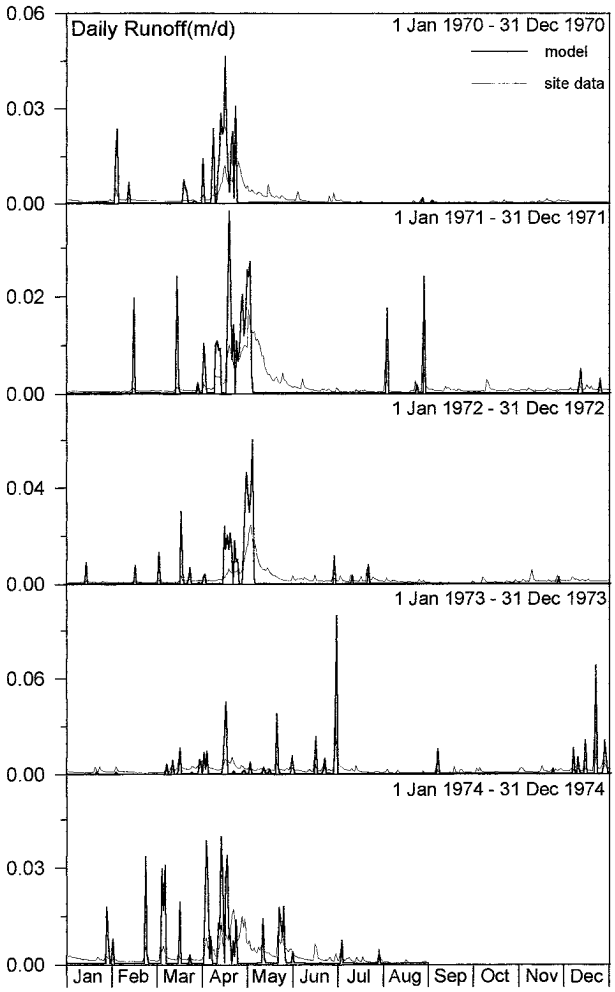

FIG. 5. Model-predicted (single column model; $K_{s,i}$ is constant with depth) daily runoff and observed runoff measured at the W-3 weir. Units are meters per second (watershed area is factored out).

simulating the growth/ablation of the snowpack. Driving the improved topographic model with the full five years of hydro-meteorological data demonstrates that not only were the ground and snow surface radiation temperatures adequately modeled, but all features of snowpack ripening that characterize snowpack growth and ablation are simulated. Figures 3 and 4 compare model results with site data for the 1970/71 snow season [see Lynch-Stieglitz (1994) for a more detailed discussion of the validation of the snow model]. However, virtually identical results are generated when driving the single-column alone (with $K_{s,i}$ constant or declining exponentially with depth). The single-column model seems to be able to capture those processes that are primarily governed by the vertical fluxes of water and energy at the plot scale. By including topographic effects we do not improve the model simulation. The same cannot be said for the simulation of such topographically controlled processes such as watershed runoff and soil moisture heterogeneity.

An appreciation for model discharge results is first obtained by examining the nature of the stream hydrograph in this New England watershed (Figs. 5–7, site weir data). The typical hydrograph is characterized by a relatively fast rising limb to peak discharge values (surface runoff) and a slow recession toward nominal values (baseflow). Surface runoff generated over saturated regions (due to snowmelt, precipitation, or throughfall) rapidly enters the stream system. The slower baseflow resulting from the relaxation of the hydraulic gradient due to gravity carries most of the discharge. With this in mind, the deficiencies of omitting topographic control of soil moisture becomes clearer.

Single-column results show the model reproduces neither the structure of the main spring hydrographs nor individual storm hydrographs (Fig. 5). While the low-frequency time series of weir measurements is consistent with the view that baseflow dominates discharge,

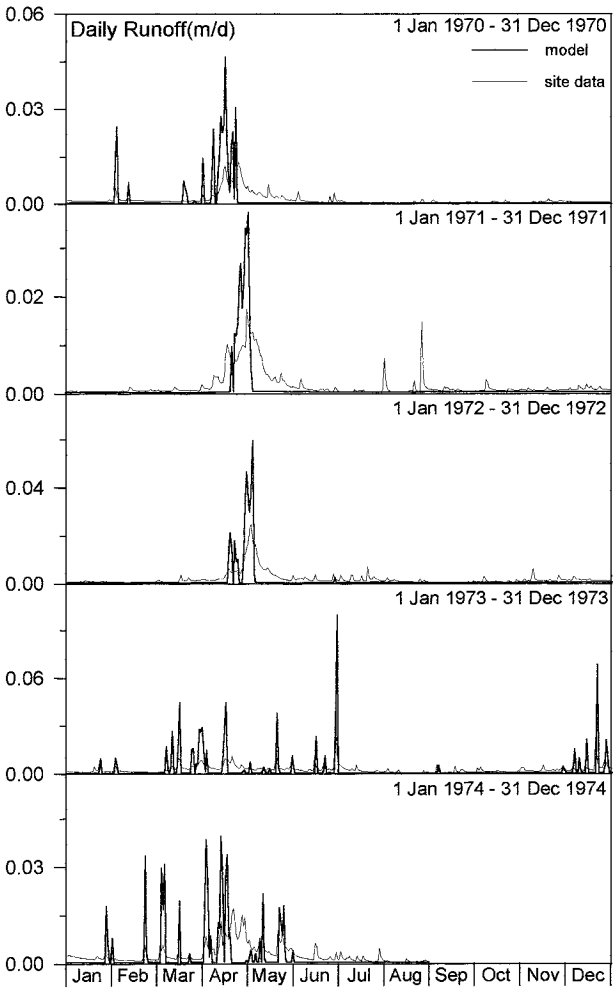

FIG. 6. Model-predicted (single column model where $K_{s,i}$ exponentially decays with depth) daily runoff and observed runoff measured at the W-3 weir. Units are meters per second (watershed area is factored out). Note: with increased near surface saturated conductivities, much of the mid-winter infiltration excess runoff seen in Fig. 5 is eliminated.

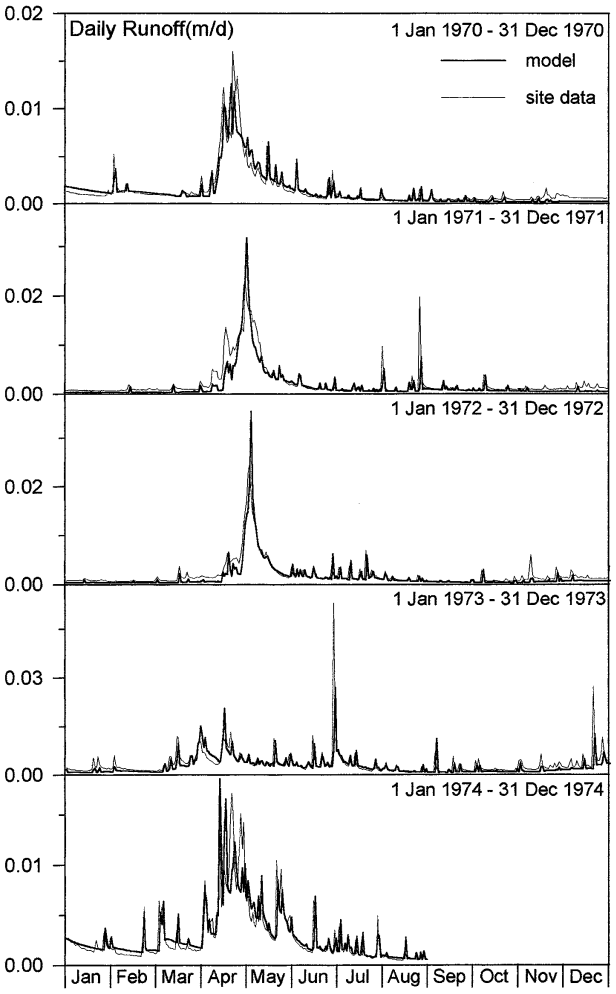

FIG. 7. Model-predicted (improved model that incorporates TOPMODEL equations) daily runoff and observed runoff measured at the W-3 weir. Units are meters per second (watershed area is factored out).

the high-frequency model results indicate that surface runoff dominates. Indeed, the mean annual model baseflow is only 20% of total model discharge (Fig. 8). By using the compacted values for the saturated conductivities of all model layers (Rawls et al. 1982) and neglecting the exponential increase of K_s toward the soil surface, infiltration excess, a runoff mechanism known to contribute insignificantly to streamflow, is responsible for 66% of total runoff (Fig. 9). It is interesting to note that while the mechanisms responsible for producing model runoff are inconsistent with reality, the overall hydroclimatology readjusts itself to give results similar to the those generated when the effects for topography are fully incorporated into the model (Figs. 10–11). Not only are the mean annual discharges for the three runs comparable (61–62 cm yr^{-1}), but the monthly climatologies of sensible and latent heat fluxes are almost identical. The reasons for this apparent paradox are discussed shortly.

As an intermediate step to fully incorporating topographic effects, the exponential decline of K_s is incorporated into the single-column model (Fig. 6). With increased near-surface saturated conductivities, much of the midwinter infiltration excess runoff is eliminated (Fig. 9). However, in the face of baseflow that increases ever so slightly from the baseline run (Fig. 8), this infiltrating water only serves to increase the overall soil moisture climatology (Fig. 10). It is the near-surface water table that is now responsible for a higher proportion of the high-frequency runoff characteristics. In short time the water table reaches the ground surface, the saturated fraction instantaneously becomes one (from a value of zero), and all surface water runs off as overland flow. This behavior is typical of bucket models. With annual surface runoff unchanged from the previous run, saturation excess runoff picks up the slack

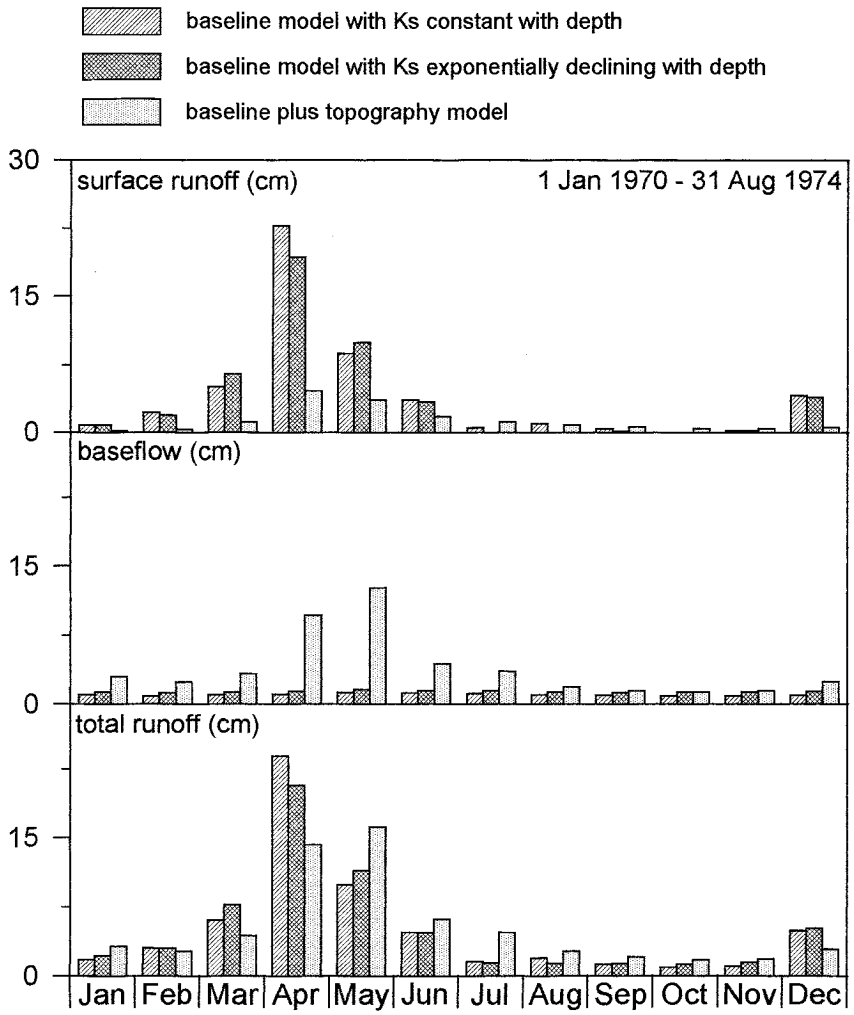

FIG. 8. Monthly averaged climatology of total model runoff is separated into its surface runoff and baseflow components.

from diminished infiltration excess runoff such that the overall hydroclimatology again readjusts to give results similar to the other runs (Figs. 10–11). Finally, with such high values of near surface saturated conductivities it might be expected that all infiltration excess runoff would be eliminated from model results. Figure 9 shows this not to be the case. As the midwinter soils fill up, the near-surface model layers freeze (Fig. 3) and severely limit further infiltration of snowpack meltwater. In these instances the water table is located in the unfrozen deeper model layers that ever so slowly generate baseflow. By not considering topographic effects, these single-column representations neither reproduce either the time history of discharge nor the correct partitioning of surface runoff and baseflow.

In the improved model that incorporates topographic effects not only are the main spring hydrographs and individual storm hydrographs adequately resolved (Fig. 7), but the mechanisms generating runoff are consistent with the hydrologic processes known to be acting in the region (Dunne and Black 1970). As the snowpack ablates in late April and May, the water table ($\bar{z}$) is recharged and rises from an autumn value of 1.5 to 0.75 m in May and the partial contributing area increases from 6.5% to 19.5% (Fig. 12). Simultaneous with the rise of the water table and expansion of lowland saturated zones are an increase in baseflow and saturation excess runoff (Figs. 8 and 9). Baseflow is now the major contributor to runoff at 76% of total discharge and saturation excess runoff is the sole contributor to surface runoff. With lower values of winter soil moisture (Fig. 10) even the fastest rates of snowpack meltwater generation can be accommodated in the soil column. After the snowpack ablation $\bar{z}$ relaxes under the influence of gravity, soil texture, and topography, and baseflow slowly decays into the summer months. Evapotranspiration (and the latent heat flux) picks up in early May, peaks in July/August and falls off as the snow season ap-

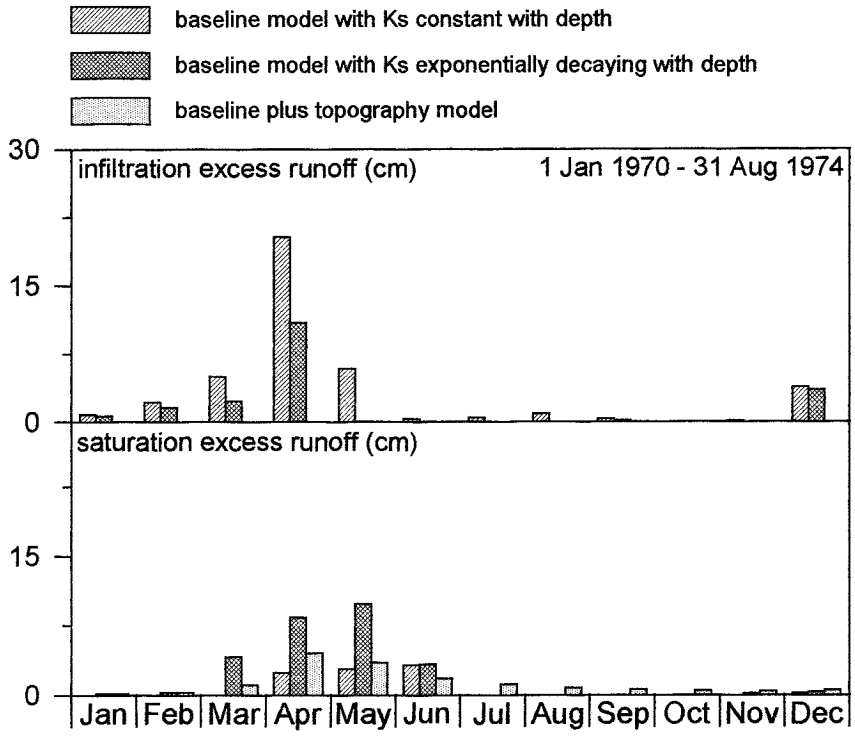

FIG. 9. Monthly averaged climatology of total surface runoff separated into its saturation excess and infiltration excess components.

proaches. During the snow-covered winter months the sensible heat flux is into the terrestrial landscape, and the relatively wet soil column results in a low Bowen ratio of 0.04 during summer months.

For the years 1970–74, topographic model results yield a mean, maximum, and minimum value of 10.4%, 42%, and 3.8% for the partial contributing area. The monthly climatology of the movement of the mean water table ($\bar{z}$, Fig. 12) and the mean annual volumetric soil moisture for the root zone, at 36%, is much more consistent with neutron probe data taken at three locations throughout W-3 covering the years 1963–69 (Anderson 1977) than model results with the single-column model alone. Finally, for the period 1970–74, the mean annual precipitation of 125 cm and discharge of 73 cm measured at W-3 yields a balance of 52 cm for evapotranspiration when the assumption is made of zero annual soil moisture change. Model generated results yield 62 cm for discharge and 63 cm for evapotranspiration.

As stated earlier, while the mechanisms responsible for producing model runoff with the single-column model alone are inconsistent with reality, the overall hydroclimatology readjusts to give surface fluxes similar to the those generated when the effects for topography are fully incorporated into the model (Fig. 11). With its high precipitation, low-evaporative demand and rolling hills, Sleepers River offers an unstressed environment (even in summer) for vegetation. The fact that the roots always have easy access to a relatively nearby water table allows for transpiration at or near the potential rate. As such, a GCM modeler only concerned with the generation of surface fluxes to the atmosphere would find that topographic effects at Sleepers River play only a minimal role in this regard. However, if the concern is the soil moisture generated by the model or the flux of water through the soil column that will transport dissolved organic carbon (Hornberger et al. 1994) and nutrients out of the soil column and into the stream system, topographic effects must be included. Further, if an eventual goal of GCM modeling is to include for trace gas fluxes of CO_2 and methane, then topographic effects must be included in that the fluxes of both are significantly different between the saturated lowlands and the drier uplands. The approach taken in this paper allows one to dynamically track both the expansion and contraction of these lowland saturated zones and the state of the upland soil moisture.

The above results suggest that the correct partitioning of evapotranspiration and total runoff in a land-surface model does not require the more sophisticated treatment of topography that is demonstrated here. However, in drier regions, where the evaporative demand cannot be satisfied everywhere, topography will have a large impact on evapotranspiration, and thus the partitioning of latent and sensible heat [see, e.g., Famiglietti and Wood (1994a,b) for an example at the FIFE site]. In these regions, where evapotranspiration occurs at the potential rate only in the small saturated portions of the water-

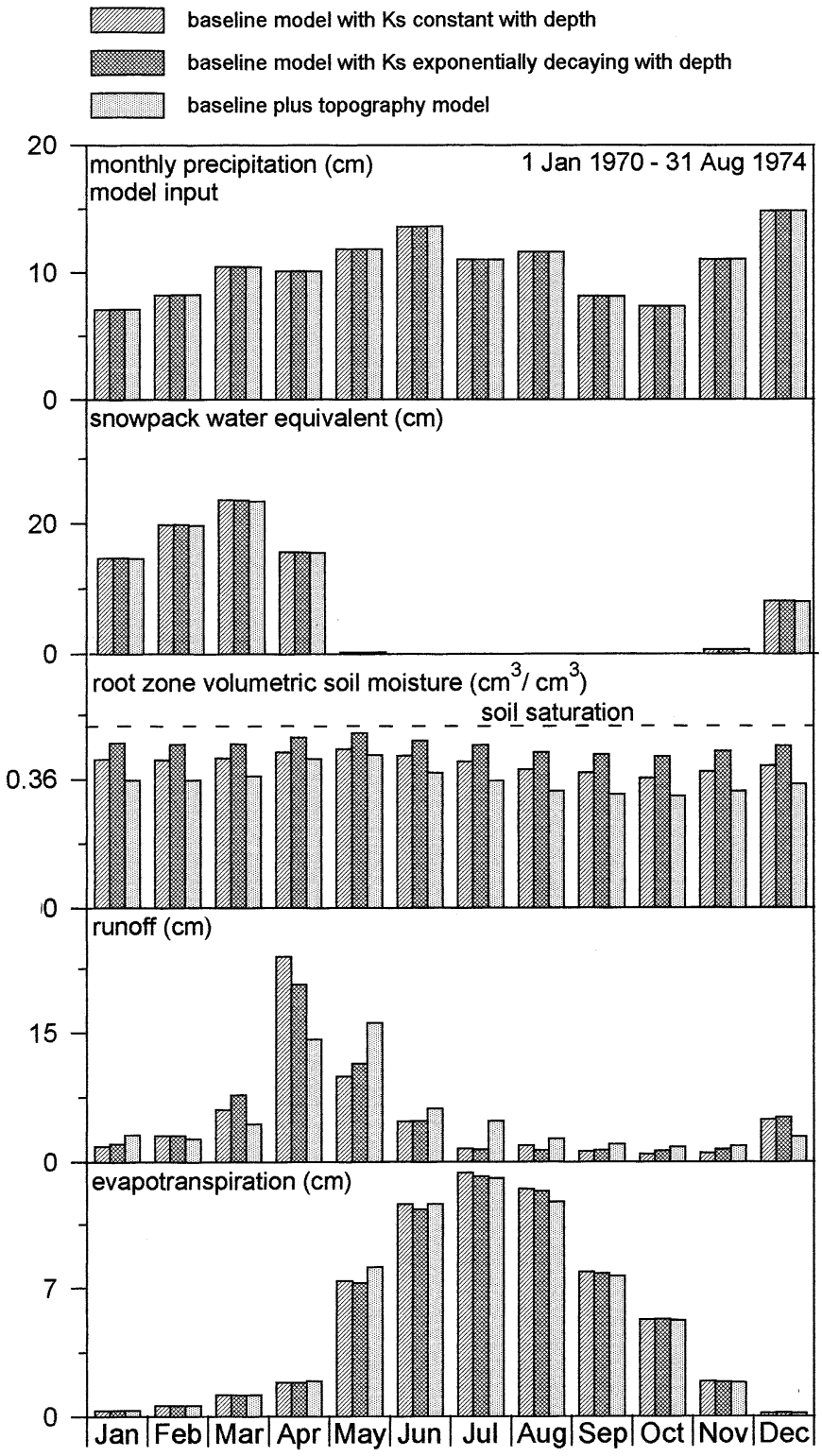

FIG. 10. Monthly averaged climatology of the watershed water balance components.

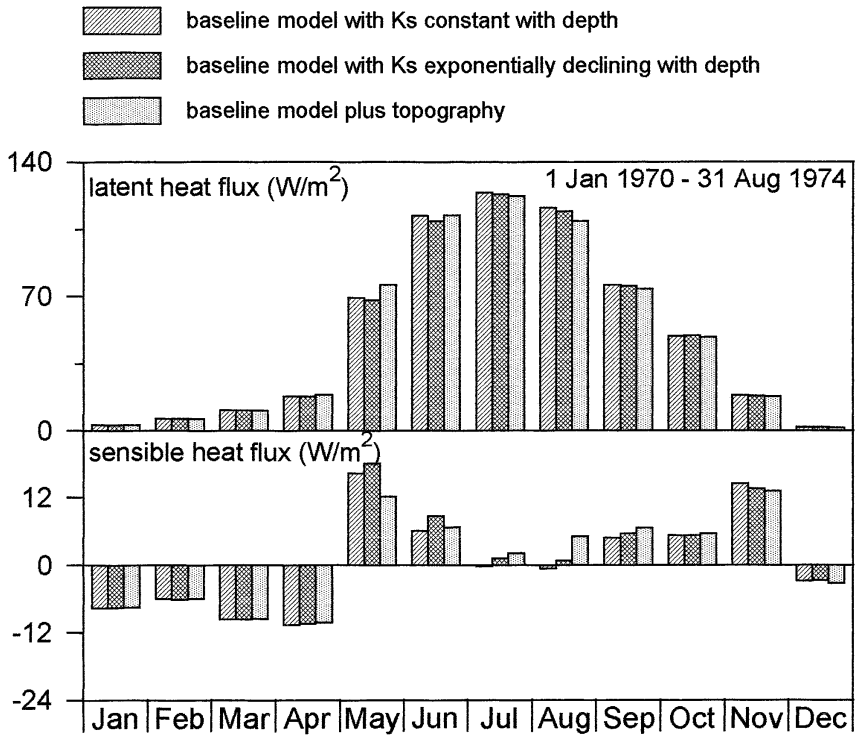

FIG. 11. Monthly averaged climatology of the watershed energy balance components (latent and sensible heat fluxes).

shed, the single-column model will, again, retain enough soil moisture such that the lack of sufficient baseflow may this time be compensated by unrealistically enhanced evapotranspiration. So while the inclusion of topographic effects may not affect the modeled partitioning between total runoff and evapotranspiration in a wet climate such as Sleepers River, this partitioning would be much more sensitive to the parameterization of topography in a drier climate.

5. Conclusions

The current generation of land-surface models used in GCMs view the soil column as the fundamental hydrologic unit. While this may be effective in simulating such processes as the evolution of ground temperatures and the growth/ablation of a snowpack at the soil plot scale, it effectively ignores the role topography plays in the development of soil-moisture heterogeneity and the subsequent impacts of soil-moisture heterogeneity on watershed evapotranspiration and the partitioning of surface fluxes. This approach also ignores the role topography plays in the timing of discharge and the partitioning of discharge into surface runoff and baseflow. In this paper we present an approach to land-surface modeling that allows us to view the watershed as the fundamental hydrologic unit. The analytic form of TOPMODEL equations are coupled with a single-column model framework and the resulting model is used to predict the saturated fraction of the watershed and baseflow in a consistent fashion. Soil moisture heterogeneity represented by saturated lowlands subsequently impacts the partitioning of surface fluxes, including evapotranspiration and runoff. The approach is computationally efficient, allows for a greatly improved simulation of the hydrologic cycle, and is easily coupled into the existing framework of the current generation of single-column land-surface models. Because this approach uses the statistics of the topography rather than the details of the topography, it is compatible with the large spatial scales of today's regional and global climate models.

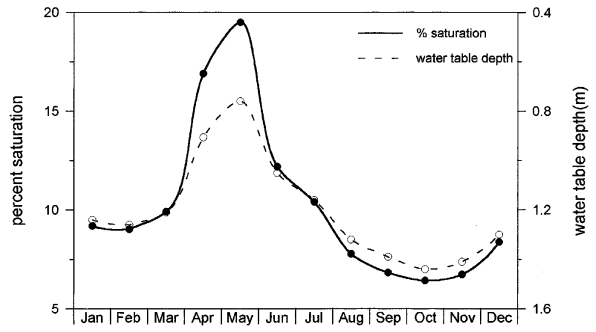

FIG. 12. Monthly averaged climatology of the mean water table depth ($\bar{z}$) and the percent of watershed saturated (partial contributing area).

The study of current and changed climates covering

a wide range of climatic regimes requires a physically based model that will have the flexibility to deal with different conditions, whereas the spatial scales of regional and global climate models demand a computationally efficient model. As the availability and familiarity of DEM data increases, the approach presented here will allow the GCM modeler to more realistically represent land-surface processes without the need to resort to finite-element modeling. Finally, because this approach allows us to track the expansion and contraction of lowland saturated zones, the state of the upland soil moisture, and the baseflow consistent with the saturated fraction, we now have a logical framework to realistically deal with such issues as the movement of nutrients from the hillslope to the streams, rivers, and ulimately the oceans and the terrestrial–atmosphere fluxes of trace gases.

Acknowledgments. We thank Dave Wolock for supplying the topography statistics for the Sleepers River watershed and his many helpful discussions regarding TOPMODEL, as well as Jamey Shanley for discussions on the watershed itself. We also thank E. Anderson at the National Weather Service Hydrologic Research Laboratory, R. Dekett at the USDA Soil Consevation Service, T. Pangburm at the Cold Regions Research and Engineering Laboratory, and J. Thurman at the USDA-ARS Hydrology Laboratory for supplying the datasets and soil maps used in this study. The time and effort Tim Pangburm took out of his own schedule to compile the necessary hydro-meteorological data into an easy format is especially appreciated. Finally, We thank Z.-.L Yang for supplying that portion of the BEST code that is responsible for canopy calculations. This work was supported by The U.S. Environmental Protection Agency office of Exploratory Research and office of Policy, Planning, and Evaluation, Global Climate Change Division.

REFERENCES

Abramopoulos, F., C. Rosenzweig, and B. Choudhury, 1988: Improved ground hydrology calculations for global climate models (GCMs): Soil water movement and evapotranspiration. *J. Climate,* **1,** 921–941.

Anderson, E. A., 1967: Estimating incident terrestrial radiation under all atmospheric conditions. *Water Resour. Res.,* **3,** 975–988.

——, 1976: A point energy balance model of a snow cover. Office of Hydrology, National Weather Service, NOAA Tech. Rep. NWS 19, 150 pp.

——, 1977: NOAA-ARS cooperative snow research project—Watershed hydro-climatology and data for water years 1960–1974. NOAA Tech. Rep., NOAA-S/T 77-2854, 316 pp.

Bell, K. R., B. J. Blanchard, T. J. Shmugge, and M. W. Witczk, 1980: Analysis of surface moisture variations in large-field sites. *Water Resour. Res.,* **16,** 796–810.

Beven, K. J., 1982a: Macropores and water flow in soils. *Water Resour. Res.,* **18,** 1311–1325.

——, 1982b: On subsurface stormflow: An analysis of response times. *Hydrol. Sci. J.,* **27,** 505–521.

——, 1984: Infiltration into a class of vertically non-uniform soils. *Hydrol. Sci. J.,* **29,** 425-434.

——, 1986a: Hillslope runoff processes and flood frequency characteristics. *Hillslope Processes,* A. D. Abrahams, Ed., Allen and Unwin, 187–202.

——, 1986b: Runoff production and flood frequency in catchments of order n: An alternative approach. *Scale Problems in Hydrology,* V. K. Gupta, I. Rodriguez-Iturbe, and E. F. Wood, Eds., D. Reidel, 107–131.

——, and M. J. Kirkby, 1979: A physically-based variable contributing area model of basin hydrology. *Hydrol. Sci. J.,* **24,** 43–69.

——, P. Quinn, R. Romanowicz, J. Freer, J. Fisher, and R. Lamb, 1994: TOPMODEL and GRIDATB, A users guide to the distribution versions (94.01). Tech Rep. TR110/94, Centr. for Res. on Environ. Syst. and Stat., Lancaster University, Lancaster, U.K.

Boer, G. J., N. A. McFarlane, R. Laprise, J. D. Henderson, and J.-P. Blanchet, 1984: The Canadian Climate Centre spectral atmospheric general circulation model. *Atmos. Ocean,* **22,** 397–429.

Brooks, R. H., and A. T. Corey, 1964: Hydraulic properties in porous media, Colorado State University, Fort Collins, CO, 27 pp.

Burt, T. P., and D. P. Butcher, 1985: Topographic controls of soil moisture distributions. *J. Soil Sci.,* **36,** 469–486.

Calder, I. R., 1990: *Evaporation in the Uplands.* Wiley, 148 pp.

——, 1993: Hydrologic effects of land-use change. *Handbook of Hydrology,* D. R. Maidment, Ed., McGraw-Hill, 13.1–13.49.

Charney, J.G., 1975: Dynamics of deserts and drought in the Sahel. *Quart. J. Roy. Meteor. Soc.,* **101,** 193–202

——, W. K. Quirk, S.-H. Chow, and J. Kornfield, 1977: A comparative study of the effects of albedo changes on drought in semi-arid regions. *J. Atmos. Sci.,* **34,** 1366–1385.

Da Silva, C. C., and E. De Jong, 1986: Comparison of two computer models for predicting soil water in a tropical monsoon climate. *Agric. For. Meteor.,* **36,** 249–262.

Deardorff, J. W., 1978: Efficient prediction of ground surface temperature and moisture with inclusion of a layer of vegetation. *J. Geophys. Res.,* **83,** 1889–1903.

Dickinson, R. E., A. Henderson-Sellers, P. J. Kennedy, and M. F. Wilson, 1986: Biosphere-Atmostphere Transfer Scheme (BATS) for the NCAR Community Climate Model. NCAR Tech. Note NCAR/TN-275+STR, 69 pp.

Dunne, T., and R. D. Black, 1970: Partial area contributions to storm runoff in a small New England watershed. *Water Resour. Res.* **6,** 1297–1311.

Elsenbeer, H., K. Cassel, and J. Castro, 1992: Spatial analysis of soil hydraulic conductivity in a tropical rainforest catchment. *Water Resour. Res.,* **28,** 3201–3214.

Entekhabi, D., and P. S. Eagleson, 1989: Land surface hydrology parameterization for atmostpheric general circulation models including subgrid-scale spatial variability. *J. Climate,* **2,** 816–831.

Famiglietti, J. S., and E. F. Wood, 1991: Evapotranspiration and runoff from large land areas: Land surface hydrology for Atmospheric General Circulation Models. *Surv. Geophys.,* **12,** 179–204.

——, and ——, 1994a: Multiscale modeling of spatially variable water and energy balance processes. *Water Resour. Res.,* **30,** 3061–3078.

——, and ——, 1994b: Application of multiscale water and energy balance models on a tallgrass prairie. *Water Resour. Res.,* **30,** 3079–3093.

FAO-UNESCO, 1974: *Soil Map of the World 1:5,000,000.* UNESCO.

Freeze, R. A., 1974: Streamflow generation. *Water Resour. Res.,* **12,** 627–647.

Gardner, W. R., and D. Hillel, 1962: The relation of external evaporative conditions to the drying of soils. *J. Geophys. Res.,* **67,** 4319–4325.

Hansen, J. E., G. Russel, D. Rind, P. H. Stone, A. A. Lacis, S. Lebedeff, R. Ruedy, and L. Travis, 1983: Efficient three dimensional global models for climate studies: Models I and II. *Mon. Wea. Rev.,* **111,** 609–662.

Hewlett, J. D., and R. A. Hibbert, 1965: Factors affecting the response of small watersheds to precipitation in humid areas. *Proc., Int. Symp. on Forest Hydrology*, University Park, PA, Pennsylvania State University.

Hillel, D., 1977: Computer simulation of soilwater dynamics: A compendium of recent work. International Development Research Centre, Ottawa, ON, Canada, 214 pp.

Hornberger, G. M., K. E. Bencala, and D. M. McKnight, 1994: Hydrological controls on dissolved organic carbon during snowmelt in the Snake River near Montezuma, Colorado. *Biogeochemistry,* **25,** 147–165.

Koster, R. D., and M. J. Suarez, 1992: A comparitive analysis of two land surface heterogeneity representations. *J. Climate,* **5,** 1379–1390.

Lean, J., and D. A. Warrilow, 1989: Simulation of the regional climatic impact of Amazon deforestation. *Nature,* **342,** 411–413.

Lindroth A., 1985: Canopy conductance of coniferous forests related to climate. *Water Resour. Res.,* **21,** 297–304.

——, 1993: Aerodynamic and canopy resistance of short-rotation forest in relation to leaf area index and climate. *Bound.-Layer Meteor.,* **66,** 265–279.

Liston, G. E., Y. C. Sud, and E. F. Wood, 1994: Evaluating GCM land surface hydrology parameterizations by computing river discharges using a runoff model: Application to the Mississippi Basin. *J. Appl. Meteor.,* **33,** 394–405.

Lynch-Stieglitz, M., 1994: The development and validation of a simple snow model for the GISS GCM. *J. Climate,* **7,** 1842–1855.

——, 1995: The development and validation of a new land surface model for regional and global climate modeling. Ph.D. thesis, Columbia University, 89 pp.

Manabe, S., and R. T. Wetherald, 1987: Large scale changes of soil wetness induced by an increase in atmospheric carbon dioxide. *J. Atmos. Sci.,* **44,** 1211–1235.

McFarlane, N., and R. Laprise, 1985: Parameterization of sub-grid scale processes in the AES/CCC Spectral G.C.M., Canadian Climate Centre Rep. 85-12, CCrn 17, 70 pp.

Miller, J. R., and G. L. Russell, 1992: The impact of global warming on river runoff. *J. Geophys. Res.,* **97,** 2757–2764.

——, ——, and G. Caliri, 1994: Continental scale river flow in climate models. *J. Climate,* **7,** 914–928.

Monteith, J. L., 1975a: *Vegetation and the Atmosphere.* Vol. 1, *Principles.* Academic Press, 278 pp.

——, 1975b: *Vegetation and the Atmosphere.* Vol. 2, *Case Studies.* Academic Press, 439 pp.

Owe, M., E. B. Jones, and T. J. Schmugge, 1982: Soil moisture variation patterns observed in Hand County, South Dakota. *Water Resour. Bull.,* **18,** 949–954.

Pitman A. J., and C. E. Desborough, 1996: Brief description of bare essentials of surface transfer and results from simulations with HAPEX-MOBILHY data. *Global Planet. Change,* **13,** 135–144.

——, Z.-L. Yang, J. G. Cogley, and A. Henderson-Sellers, 1991: Description of bare essentials of surface transfer for the bureau of meteorological research centre AGCM, BMRC, Australia. BMRC Research Rep. 32.

Quinn, P., K. Beven, and R. Lamb, 1995: The *ln(a/tan β)* index: How to calculate it and how to use it within the TOPMODEL framework. *Hydrol. Process,* **9,** 161–182.

Rawls, W. J., and D. L. Brakensiek, 1985: Prediction of soil water properties for hydrologic modeling. *Watershed Management in the Eighties,* E. B. Jones, Ed., ASCE, 293–299.

——, ——, and K. E. Saxton, 1982: Estimation of soil water properties. *Trans. ASAE,* **25** (5), 1316–1320, 1328.

Rind, D., R. Goldberg, J. Hansen, C. Rosenzweig, and R. Ruedy, 1990: Potential evaporation and the likelihood of future drought. *J. Geophys. Res.,* **95,** 9983–10 004.

Ripley, E. A., and R. E. Redman, 1975: Grassland. *Vegetation and the Atmosphere.* Vol. 2, *Case studies,* J. L. Monteith, Ed., Academic Press, 439 pp.

Shuttleworth, W. J., 1989: Micrometeorology of temperate and tropical forest. *Forest, Weather and Climate,* P. G. Jarvis and J. L. Monteith, Eds., The Royal Society, 173–436.

Sivapalan, M., K. Beven, and E. F. Wood, 1987: On hydrologic similarity. 2, A scaled model of storm runoff production. *Water Resour. Res.,* **23,** 2266–2278.

Stewart, J. B., and A. S. Thom, 1973: Energy budgets in pine forest. *Quart. J. Roy. Meteor. Soc.,* **99,** 154–170.

Szeicz, G., and I. F. Long, 1969: Surface resistance of crop canopies. *Water Resour. Res.,* **5,** 622–633.

USDA, 1993: Soil Conservation Service, Caledonia County, Vermont, soil maps of the W-3 watershed and soil interpretation records.

Verseghy, D.L., 1991: CLASS—A Canadian Land Surface Scheme for GCMS. I: Soil model. *Int. J. Climatol.,* **11,** 111–133.

Wang, J. R., T. J. Schmugge, J. C. Shiue, and E. T. Engman, 1989: Mapping surface soil moisture with L-band radiometric measurements. *Remote Sens. Environ.,* **27,** 305–312.

Wolock, D. M., and C. V. Price, 1994: Effects of digital elevation model map scale and data resolution on a topography-based watershed model. *Water Resour. Res.,* **30,** 3041–3052.

——, and G. J. McCabe Jr., 1995: Comparison of single and multiple flow direction algorithms for computing topographic parameters in TOPMODEL. *Water Resour. Res.,* **31,** 1315–1324.

Wood, E. F., M. Sivapalan, and K. Beven, 1990: Similarity and scale in catchment storm response. *Rev. Geophys.,* **28,** 1–18.

Zhang, W., and D. R. Montgomery, 1994: Digital elevation model grid size, the landscape representation, and hydrologic simulations. *Water Resour. Res.,* **30,** 1019–1028.